Effect of Trap on Carrier Transport in InAs FET with Al_2O_3 Oxide: DFT-based NEGF simulations

Mincheol Shin
School of Electrical Engineering
Korea Advanced Institute of Science and Technology
Daejeon 34141, Republic of Korea
mshin@kaist.ac.kr

Yucheol Cho
School of Electrical Engineering
Korea Advanced Institute of Science and Technology
Daejeon 34141, Republic of Korea
yc_cho@kaist.ac.kr

Seonghyeok Jeon
School of Electrical Engineering
Korea Advanced Institute of Science and Technology
Daejeon 34141, Republic of Korea
jsh7700@kaist.ac.kr

***Abstract*— To accurately assess the effect of trap on the performance of field effect transistors (FETs), atom-level first-principles modeling of channel/oxide/trap and rigorous quantum mechanical transport calculations are necessary. In this work we have developed an innovative approach to solve the challenging problem efficiently. Non-equilibrium Green's function simulation of InAs FET with a trap in the channel/oxide interface that is atomically modeled by using the density functional theory is demonstrated.**

Keywords*— *Non-equilibrium Green's function, Density functional theory, Defect/trap, III-V channel material, field effect transistor

I. Introduction

As the feature size of the field effect transistors (FETs) approaches a few nanometer scale, it has become increasingly important to simulate the devices at the atomistic level. While the empirical tight-binding method seems suited for atomistic modeling, it has many limitations, especially when heterostructure with interface and trap is involved. First-principles density functional theory (DFT) which does not rely on empirical parameters would give an ultimate solution. But the great hurdle in utilizing DFT Hamiltonians is that the size of the non-orthogonal Hamiltonian matrices becomes prohibitively large for transport simulations of realistically sized devices.

A scheme to overcome the computational hurdle [1,2] has been introduced recently and its applications to homojunction devices were demonstrated [3]. In the approach, the DFT and non-equilibrium Green's function method (NEGF) parts are separated, where the latter method is used for electron transport calculation in the device region. Namely, one calculates the electronic structure of the unit cell by the DFT method, repeats the unit cell to construct the device region with source and drain regions attached, and implements the NEGF transport calculations for the device using the imported DFT Hamiltonians of the unit cell. Then using the mode space transformation, the Hamiltonian is reduced in size without any practical loss in accuracy in terms of device simulation outputs. In this work, the approach is extended to include an interface trap in the channel region. An oxide trap which gives rise to a defect state within the band gap is particularly paid attention to because it is expected to provide a leakage path affecting subthreshold current.

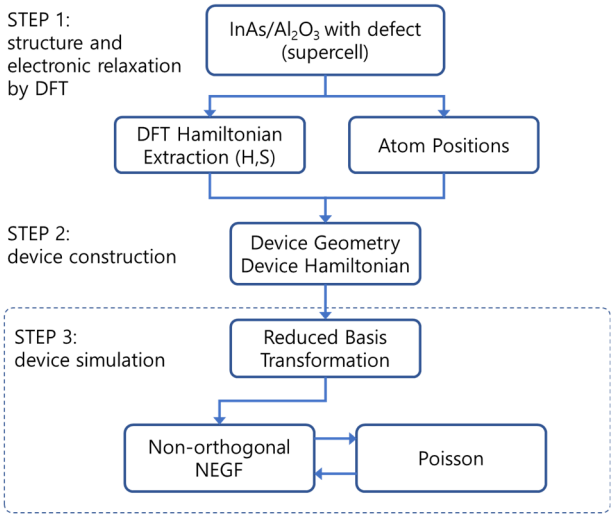

Fig. 1: Simulation flowchart. Simulations are performed in the three stages: density functional theory (DFT) relaxation of supercell, followed by the extraction of Hamiltonian and construction of the device region. After Hamiltonian matrices are effectively reduced, they are fed to the NEGF-Poisson self-consistent calculation. Upon convergence, current is calculated.

II. DFT Modeling

The overall simulation flow is shown in Fig. 1. Firstly, linear combination of atomic orbitals based DFT structural relaxations and band structure calculations were performed by using SIESTA tool [4]. PSML norm-conserving pseudopotentials [5] were used to obtain transferable results as practiced with the plane-wave based DFT. The generalized gradient approximation (GGA) and Perdew, Burke and Ernzerhof exchange (PBE) functional were employed. The band gap underestimation of GGA-PBE were adjusted by using the DFT-1/2 technique [6]. For the bulk InAs, the DFT-1/2 scheme opens the band gap of 0.42 eV which agrees well with the experimental result [7].

Atomic configuration of the defect-free $InAs/Al_2O_3$ structure is shown in Fig. 2 (a). The crystalline α-Al_2O_3 was considered for the oxide, which was strained to match the lattice constant of InAs. As-O bonds were formed at the interface to mimic the As-rich condition usually practiced in the experiments [8].

978-1-7281-0940-4/19/$31.00 ©2019 IEEE

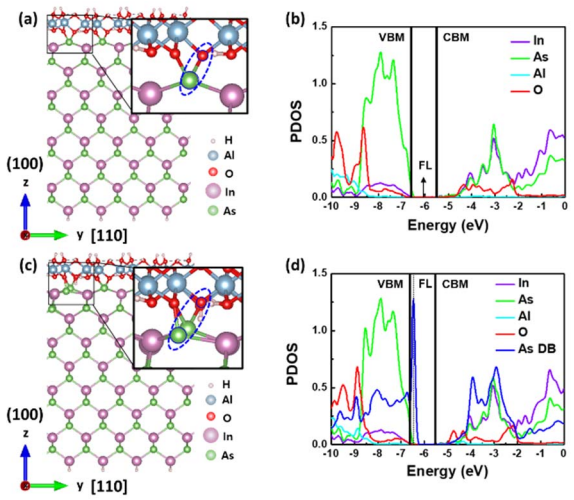

Fig. 2: (a) Atomic configuration of the defect-free $InAs/Al_2O_3$ cell with an As-O bond magnified. (b) Projected density of state (PDOS) of the supercell (a) where the Fermi level (FL) is located in the middle of the band gap. (c) Atomic configuration of the $InAs/Al_2O_3$ cell with a broken As-O bond resulting an As dangling bond. (d) PDOS of (c) where the defect energy state is shown as the sharp peak close to the valence band maximum (VBM).

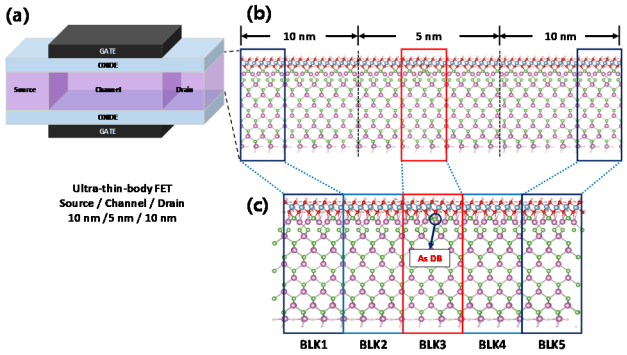

Fig. 3: (a) Schematic diagram of ultrathin-body InAs simulated in this work. The source/channel/drain regions modelled atomically are shown in (b), which are constructed by using the blocks of the relaxed DFT supercell shown in (c). BLK3 contains an As DB while BLK1 and BLK5 are very close to standalone, pure $InAs/Al_2O_3$ unit cell. The latter two are used as the source and drain blocks and also as the blocks to fill up the rest of the device region besides the block containing the trap and its neighbor blocks.

A defect at the interface was created when an As-O bond was broken resulting an As dangling bond (DB) and hydrogen passivated oxygen. See Fig. 2 (c). The supercell containing the defect is shown in Fig. 3 (c), which has the thickness of 22.54 Å in the z direction and periodically repeated in the x and y directions. The As DB is positioned in the middle block (BLK3) which is sided by defect-free $InAs/Al_2O_3$ blocks (BLK2 and BLK4) to ensure no interaction between the defect and its periodic images. BLK1 and BLK5 are very close, in terms of the geometric and electronic structures, to the standalone, pure $InAs/Al_2O_3$ unit cell. Each block in the figure has the size of 3x4 primitive cells or 13.14 Å by 17.51 Å and contains the total of 360 atoms (361 atoms for BLK3). The block size was chosen to guarantee the nearest neighbor interaction condition between neighboring blocks (and between the blocks and their periodic images) as each block is to be used as an unit cell in the NEGF transport calculation in the followings.

Figs. 2 (b) and (d) show the projected density of state (PDOS) of the defect-free and the structure with an As DB, respectively. As shown in the figures, the As DB gives rise to a sharp defect energy state above and close to the valence band maximum (VBM) and as the consequence the Fermi level becomes located close to the defect energy state. Fig. 4 shows the band diagrams of the two structures, where the flat defect state is clearly seen in the right panel. The Fermi level indicated in the figure is the one of the entire supercell of Fig. 3 (c). Thus it may be estimated that the defect energy states lies about 0.06 eV above the VBM of the defect free structure. It is just an estimation because the band diagram of the right panel of Fig. 4 corresponds to the case where BLK3 is repeated periodically, which is obviously not the case for the actual BLK3 which is a part of the supercell shown in Fig. 3 (c).

III. NEGF TRANSPORT CALCULATION

After relaxation of the supercell, the nonorthogonal DFT Hamiltonian and overlap matrices of the supercell were extracted and used to construct the device region as shown in Figs. 3 (a) and (b). Each block of the supercell of Fig. 3 (c) is treated as a unit cell in the transport calculation; for instance, BLK1 is repeated to construct the source region and BLK5 is repeated to construct the drain region, while the channel region is constructed by 4 blocks of BLK2, BLK3, BLK4, and BLK5. Then the As DB which acts like a trap is located about 2.0 nm from the beginning of the channel region.

The Hamiltonian size of each unit cell containing 360 (361) atoms is 5064x5064 (5069x5069), where the number between the parenthesis is for the block containing the defect. Using the scheme in Ref. [2], the Hamiltonian matrices were reduced to about 100, which is about 2% of its original size. The Hamiltonian corresponding to BLK1, BLK3, and BLK5 were reduced and their unitary transformation matrices were applied to the original device Hamiltonian. The reduced Hamiltonian size was bigger than that of homojunction systems due to the coupling of wider range of modes of hetero-cells.

For transport calculations, the Hamiltonian and overlap matrices were fed to an in-house non-orthogonal non-equilibrium Green's function (NEGF) simulator, where the hole density is given by

$$p = \int \frac{dE}{2\pi} [G^p S]_{diag}$$

where G^p is the hole Green's function matrix and S is the overlap matrix. The hole density was calculated because the p-type device was considered in this work. With the hole density, the three dimensional Poisson's equation is solved for the electrostatic potential

$$\nabla^2 \phi(\vec{r}) = -\frac{q_0}{\epsilon}(p(\vec{r}) - N_A)$$

where ϵ is the permittivity and N_A is the doping density. Upon the convergence of the self-consistent calculation between the hole density and the electrostatic potential, the current was calculated. Ballistic transport was assumed. To account for the discrete nature of atoms, the finite element method was used to solve the Poisson's equation.

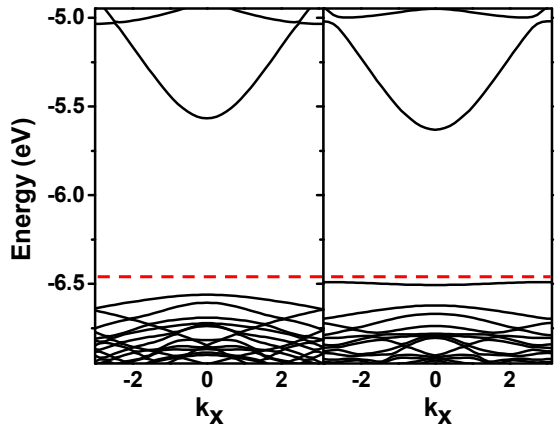

Fig. 4: (Left) The band diagram of the defect-free cell. (Right) The band diagram of the cell with an As DB as described in the text. The dashed line represents the Fermi level of the whole structure shown in Fig. 3 (c). The band diagrams are for $k_y = 0$ where k_y is the wave vector in the transverse (y) direction. Note that the unit cell structures assume the periodicity in the y direction, with the periodicity of $4u_y$ where u_y is the width of the primitive unit cell. As mentioned in the text, there are 3x4 primitive cells in the unit cells.

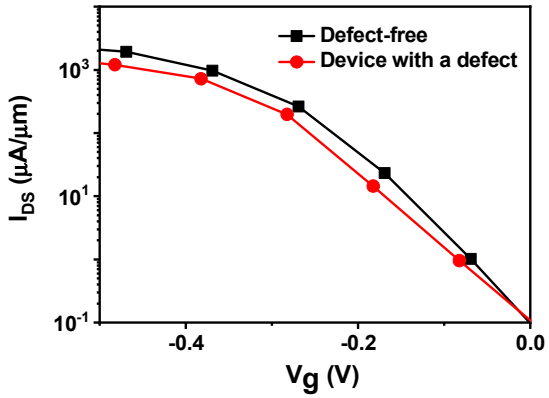

Fig. 6: Current-voltage characteristics of the simulated p-type UTB devices with 5.25 nm channel length and 2.25 nm channel width. The device with an As DB in the channel region (red line with circles) and the defect-free device (black line with squares) are compared. The OFF state current of 0.1 $\mu A/\mu m$ is assumed and the curves are adjusted accordingly. The drain voltage of -0.5 V is applied. The device with the defect shows the subthreshold swing of 85 mV/decade while the defect-free device shows 74 mV/decade. The ON currents are 2130 $\mu A/\mu m$ and 1280 $\mu A/\mu m$, respectively, for the defect-free and the device with defect.

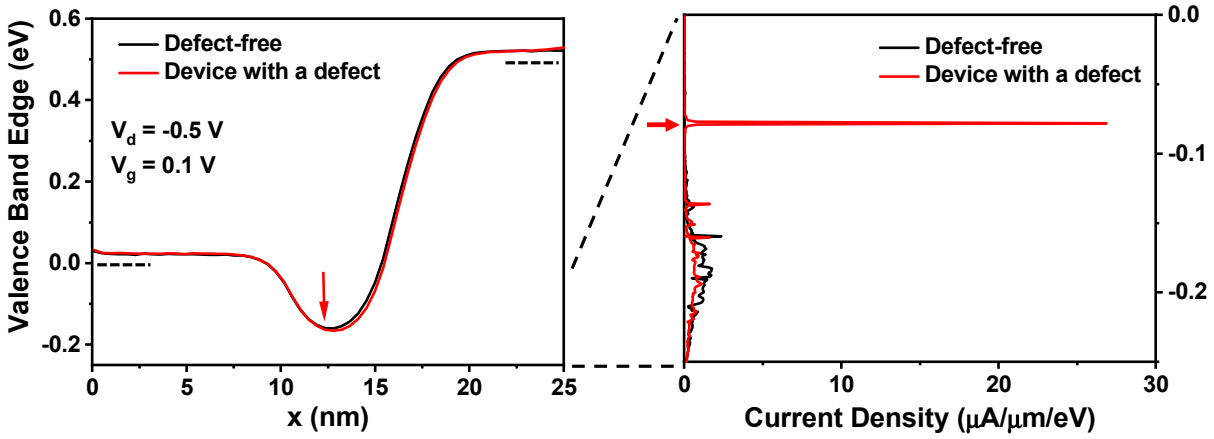

Fig. 5: The valence band edge profile for the p-type InAs FET shown in Fig. 3 and the corresponding energy-resolved current density. Black and red lines are for defect-free device and the device with an As DB in the channel (its location indicated as arrow in the left panel), respectively. In the current density graph, the peak due to tunneling current through the trap is indicated by the arrow.

IV. Device Simulation

Ultra-thin-body (UTB) double-gate InAs FET is constructed as shown in Fig. 3 (b) using the blocks of Fig. 3 (c). InAs in the channel region is 2.25 nm thick, and 1 nm thick oxide consists of minimum layers of actual Al_2O_3 atoms to keep intact the band structure of InAs/Al_2O_3 and virtual atoms to fill up the rest of the oxide region. The bulk dielectric constants of 15 and 20 are assumed for channel and oxide, respectively. The source and channel regions are 10.5 nm long each and the channel length is 5.25 nm.

Since the defect state lies close to VBM, a p-type UTB transistor has been simulated to demonstrate the effect of the trap on the transport properties; the source and drain regions are assumed to be p-doped with the doping density of $10^{20}\ cm^{-3}$. To account for the periodicity in the transverse (y) direction, 12 transverse modes (k_y) are selected for the transport calculation, each of which acts as an independent channel. The drain voltage of -0.5 V is applied.

Fig. 5 shows the valence band profile of the simulated device. For comparison, the device with the same geometry but without the trap is also simulated. It is seen that, as the gate electric field is weakened due to the presence of the trap, whose location is pointed by an arrow in the figure, the potential becomes slightly higher (negatively) in the channel region. The energy resolved current density shown in Fig. 5 clearly shows the peak due to the tunneling through the trap state. The current density was calculated for the case of $k_y = 0$.

The leakage current through the defect state leads to deterioration of the subthreshold swing. Fig. 6 shows the current-voltage characteristics of the simulated p-type UTB devices where the defect-free device and the device with an

As DB are compared. The curves are adjusted such that the OFF state current is 0.1 $\mu A/\mu m$. The subthreshold swing (SS) increases significantly: SS increases from 74 mV/decade for the defect-free device to 85 mV/decade for the device with defect in the channel. As a consequence, the ON current drops to 1280 $\mu A/\mu m$ from 2130 $\mu A/\mu m$.

V. Conclusions

We have performed a rigorous DFT based NEGF simulation on ultra-thin-body InAs double-gate FET with an interface trap modeled by an As dangling bond. We have demonstrated that the device performance becomes significantly degraded by the presence of defect in the channel, due to the trap-assisted leakage tunneling current that takes place in the subthreshold region.

Acknowledgment

This work has been supported by the project SRFC-TA1703-10 under Samsung Research Funding & Incubation Center for Future Technology.

References

[1] G. Mil'nikov et al, "Equivalent transport models in atomistic quantum wires," Phys. Rev. B, vol. 85, 035317, 2012.

[2] M. Shin et al, "Density functional theory based simulations of silicon nanowire field effect transistors," J. Appl. Phys, vol. 119, 154505, 2016.

[3] M. Shin et al, "First-principles based quantum transport simulations of nanoscale field effect transistors," 2017 IEEE International Electron Device Meeting, San Francisco, 2017.

[4] José M Soler et al, "The SIESTA method for ab initio order-N materials simulation," J. Phys.: Condens. Mat., vol. 14, pp. 2745-2779, 2002

[5] A. García, M. Verstraete, Y. Pouillon, J. Junquera, "The PSML format and library for norm-conserving pseudopotential data curation and interoperability" Computer Physics Communications 227, 51-71, 2018

[6] L. G. Ferreira et al, "Approximation to density functional theory for the calculation of band gaps of semiconductors," Phys. Rev. B, vol 78, 125116, 2008.

[7] I. Vurgaftman, J. R. Meyer, and L. R. Ram-Mohan," Band parameters for III–V compound semiconductors and their alloys", J. Appl. Phys. 89, 5815, 2001.

[8] J. Robertson et al, "Defect state passivation at III-V oxide interfaces for complementary metal–oxide–semiconductor devices," J. Appl. Phys. vol. 117, 112806, 2015.